Cellular Immunology **201,** 6–13 (2000)
doi:10.1006/cimm.2000.1637, available online at http://www.idealibrary.com on IDEAL®

Perillyl Alcohol Inhibits TCR-Mediated $[Ca^{2+}]_i$ Signaling, Alters Cell Shape and Motility, and Induces Apoptosis in T Lymphocytes

Xunbin Wei,*,† Ming-Sing Si,‡ David K. Imagawa,‡,§ Ping Ji,‡,§
Bruce J. Tromberg,*,† and Michael D. Cahalan*

**Department of Physiology and Biophysics and †Laser Microbeam and Medical Program (LAMMP), Beckman Laser Institute, University of California, Irvine, California 92697; ‡Dumont–UCLA Liver Transplant Lab, UCLA School of Medicine, Los Angeles, California 90095; and §UCI Liver Transplant Lab, UCI College of Medicine, Orange, California 92868*

Received November 5, 1999; accepted March 2, 2000

Perillyl alcohol (POH) inhibits isoprenylation and has shown anticancer and chemopreventive properties in rodent models. The mechanism that underlies the anticancer activity of POH and other isoprenylation inhibitors is unknown but has been postulated to involve decreased levels of isoprenylated Ras and Ras-related proteins. Previously we demonstrated that POH effectively inhibits human T cell proliferation *in vitro* and can prevent acute and chronic rejection in a rat cardiac transplant model. In this report, we investigate the effects of POH on T lymphocytes at the single-cell level. POH disrupts the polarized shape and motility of antigen-specific murine 1E5 T cells. Using an optical trap to position anti-CD3-coated beads in contact with 1E5 T cells, we demonstrate that POH inhibits their TCR-mediated calcium response. Furthermore, we show that POH preferentially induces apoptosis in PHA-activated human T cells as well as in 1E5 T cells.

INTRODUCTION

T lymphocytes are pivotal in the development of allograft rejection during organ transplantation. Numerous pharmacological strategies have been employed to suppress T cell activation and function (1). Current standard antirejection therapy (cyclosporine or tacrolimus) targets the inhibition of cyclophilins (calcineurin or FK506-binding protein). However, all antirejection regimens have serious adverse effects, including drug toxicity, opportunistic infections, and malignancies (2). Thus, the morbidity and mortality of current immunosuppressive therapy serve as the impetus for the discovery and development of novel and safe antirejection agents.

Monoterpenes are a class of compounds produced by plants found in many commonly consumed fruits and vegetables. Monoterpenes have been shown to inhibit the isoprenylation and/or expression of small proteins, including Ras-related G proteins, and these properties have been postulated to contribute to their anticarcinogenic effects (3–4). Perillyl alcohol (POH)[1] is a relatively nontoxic agent that has been shown to be the most promising anticancer monoterpene in preclinical models (5–7). Other isoprenylation inhibitors (more specifically, the farnesyltransferase inhibitors) have also been under investigation as chemopreventive and chemotherapeutic agents. However, their precise mechanisms have remained elusive (8).

Ras-related G proteins play important roles in T cell activation and effector function (9–11). Thus it is possible to utilize isoprenylation inhibitors to inhibit T cells in organ transplantation. Indeed, POH has been shown to decrease the levels of small isoprenylated G proteins in T cells and to inhibit T cell proliferation and IL-2 production (12). Previously, we demonstrated that POH effectively prevented rejection in a rat cardiac transplant model and that POH inhibited human T cell proliferation (13). However, the effects of POH on T cell activation and signal transduction have not been clearly defined. In this report, we study the cellular mechanisms by which POH may bring about suppression of T cell function. Specifically, we examined the effects of POH on T cell morphology and motility, TCR-mediated calcium signaling, and apoptosis in an antigen-specific murine T cell line and in human T cells.

MATERIALS AND METHODS

Cell culture. The murine hen egg lysozyme (HEL)-restricted, $CD4^+$ T cell (1E5) (14) and MHC II-restricted B cell (2PK3) hybridomas (a gift from A. Sette, Cytel) were grown in RPMI 1640 containing 10% fetal

[1] Abbreviations used: APC, antigen-presenting cell; $[Ca^{2+}]_i$, intracellular calcium concentration; CD, cytochalasin D; FPP, farnesylpyrophosphate; GGPP, geranylgeranylpyrophosphate; PHA, phytohemagglutinin; PI, propidium iodide; POH, perillyl alcohol; TCR, T cell receptor.

0008-8749/00 $35.00

bovine serum (RPMI/FBS), 10 mM Hepes, 1% NEAA, glutamine, and sodium pyruvate. Cells were maintained in a humidified incubator at 37°C with 5% CO_2, 95% air. 1E5 cells were adherent to plastic flasks at 37°C and were resuspended for collection by gentle shaking at room temperature. T cells were stimulated with anti-mouse CD3ε mAb-coated beads.

Human T lymphocytes were purified from peripheral blood from consenting healthy adult donors, as described previously (15). Briefly, venous blood was collected in heparinized tubes and diluted to 50% with RPMI 1640 containing 25 mM Hepes. This suspension was then centrifuged at 400*g* through a Ficoll–Paque density gradient (Pharmacia LKB, Piscataway, NJ) for 30 min at room temperature. The interface was removed, washed three times with RPMI containing 20% FCS, and applied to a sterile nylon wool column preequilibrated with RPMI/20% FCS, and the eluted cells were washed three times with this medium. Activated human T cells were obtained by incubating them with phytohemagglutinin (PHA, 5 μg/ml). Day 3 T cell blasts were centrifuged over Ficoll–Paque to enrich for viable cells. FACS analysis showed that 77 and 82% of the cells were $CD3^+$ T cells in the resting and activated T cell population, respectively.

Antibody coating on beads. Beads were initially coated with 100 μg/ml anti-hamster Fc IgG mAb in 25% PBS for 1 h at room temperature and then with varying concentrations of FITC-conjugated hamster anti-mouse CD3 mAb of known fluorescein/protein ratio for 1 h. Beads coated with anti-hamster IgG mAb alone did not activate T cells (0%, 0/100). The number of anti-CD3 mAb on single beads was quantified using FACS analysis to compare FITC-conjugated mAb-coated beads with a standard curve of microbeads labeled with defined numbers of fluorescein molecules (FCSC, San Juan, PR). The coating variation between beads was relatively small (typically 15% coefficient of variation). With fluorescence microscopy, the beads appeared round and uniformly fluorescent. Well-coated beads are manipulated with an optical trap and placed at either leading edge of a polarized cell or a random site on a nonpolarized cell when treated with POH.

Optical trapping. The geometry of T cell/bead contact was manipulated using a tunable, near-infrared titanium:sapphire laser producing a trapping beam at about 820 nm (16). The trapping laser was introduced via the TV port of a Zeiss laser scanning confocal microscope (LSM 410). A short-pass (720 nm) dichroic reflector was used to separate trapping and fluorescence excitation beams. A 100 $\times$ 1.3 NA Neofluor objective focused the near infrared and visible beams, resulting in 20 mW trapping power at the focal plane. This arrangement allowed trapping and fluorescence-based $[Ca^{2+}]_i$ measurements on the same cells. A wavelength of 820 nm for the optical trap was chosen to minimize cell damage (17).

$[Ca^{2+}]_i$ imaging. To measure T cell $[Ca^{2+}]_i$ on the LSM, 1E5 cells were coloaded with a combination of fura-red/AM (5 μM) and Oregon-green/AM (2 μM), two long-wavelength Ca^{2+} indicators that respond to the 488-nm excitation line of the argon laser. Cells loaded for 1.5 h at 37°C produced a red to green shift when $[Ca^{2+}]_i$ was elevated. This shift was quantified by scanning cells with the argon laser and dividing the fluorescence intensity signals from two photomultipliers with emission bands of 510–555 nm (green) and >610 nm (red). In these experiments, an anti-CD3 mAb-coated bead was held in the trap on a heated stage (37°C) and positioned so that it made contact with either leading edge of a polarized cell or with a random site of an nonpolarized cell when treated with POH. Once the cells were positioned, the trapping beam was cut off and 488-nm laser excitation was performed. A third photomultiplier collected a Ca^{2+}-insensitive blue emission band (400–480 nm) from incandescent illumination, which was used to produce a brightfield image. Scans (100–150) at 4-s intervals were made to determine whether a $[Ca^{2+}]_i$ increase occurred in the T cell following contact with the bead. T cells not responding within 400 s were scored as unresponsive. Latency of T cell $[Ca^{2+}]_i$ response was defined as a time delay between a cell–bead contact and a detectable $[Ca^{2+}]_i$ rise within the responding T cell population. $[Ca^{2+}]_i$ was estimated by dividing 488-nm-excited green and red fluorescence images pixel by pixel. A positive response was confirmed by a sharp increase in estimated $[Ca^{2+}]_i$ of at least 50% over basal levels. Calibration was performed by measuring fluorescence intensities at very low and saturating $[Ca^{2+}]_i$ in cells, using ionomycin (1 μM) and either 1 mM EGTA for R_{min} or 10 mM Ca^{2+} for R_{max}, and applying the equation of Grynkiewicz *et al.* (18).

Cell apoptosis assay. 1E5 T cells were incubated with various concentrations of POH in the mammalian Ringer solution/glucose. Activated or resting human T cells were treated with varying concentrations of POH for 18 h in complete culture medium. After POH treatment, 1E5 or human T cells were incubated for 10 min with 0.5 μg/ml FITC-conjugated annexin V and 2.5 μg/ml propidium iodide (PI; Clonetech, Palo Alto, CA) and immediately analyzed by a FACScan instrument (Becton Dickinson). Data from each experiment were analyzed on a Power Macintosh 7300/120 computer using CELLQUEST software.

Quantification of cell shape. When settled onto coverglass at room temperature, 1E5 cells adhered poorly, appeared round, and displayed few processes. However, when warmed to 37°C, these cells adhered to the glass and had a polarized appearance defined by the

shape and direction of crawling (2–5 μm/min). Before POH treatment, ~95% of T cells had a polarized shape in Ringer. To analyze cell shape, cell borders from differential interference contrast images of 1E5 cells were traced manually. A variation of the circularity-based shape index described by Donnadieu and coworkers (19) was determined by approximating the traced shape as an ellipse using Photoshop software and ratioing the long and short axes; the index of a circle is 1.0. At 37°C, 1E5 T cells had a polarized shape with a shape index of 1.3–2.0.

RESULTS

POH disrupts 1E5 T cell polarity and motility and significantly impairs the TCR-mediated $[Ca^{2+}]_i$ signal. T cell shape and motility are essential for T cell migration, activation, and effector functions. The $[Ca^{2+}]_i$ signal plays an important role in T cell activation, proliferation, and differentiation. Thus, we examined the effects of POH on these cell properties in antigen-specific murine 1E5 T cell hybridoma.

1E5 T cells have a polarized appearance defined by the shape and direction of crawling at 37°C. Their polarity, motility, and calcium response to individual antigen-presenting cells or to anti-CD3 mAb-coated bead stimulation have been well characterized in our experimental system. Using calcium imaging and an optical trap we demonstrated that 1E5 T cells were polarized antigen sensors (20, 21). T cells were 10-fold more sensitive with 5-fold shorter latency to stimulation of anti-CD3 mAb-coated beads at the leading edge compared with the tail. Furthermore, the calcium response showed an antibody-density-dependent response to anti-CD3 mAb-coated beads (21).

Incubating 1E5 T cells with POH caused a dose- and time-dependent decrease in the polarized-shaped cell population (Fig. 1B). Before POH treatment, ~95% of T cells had a polarized shape in the mammalian Ringer solution/glucose (Fig. 1A). Incubation for 30 min with 1 mM POH resulted in ~45% decrease in the polarized-shape population. Fewer than 15% of 1E5 cells had a polarized shape with 90 min incubation with 1 mM POH or 30 min incubation with 2 mM POH. Nonpolarized cells showed no motility and no calcium response to anti-CD3 mAb-coated bead stimulation (Fig. 2A). Furthermore, the rounded-up cells exhibited apoptosis-like morphology (Fig. 1C). Within the polarized-shape population, the percentage of cells with calcium response was reduced by 50% compared with that of no drug treatment (Fig. 2A). Interestingly, the latencies of calcium response have consistent 3-min increases (Fig. 2B). A possible consequence of the increased latency time is that probing naïve T cells are less likely to be successfully activated by APCs in crowded peripheral lymphoid tissue or allografts. In the complete culture medium, 1E5 cells did not round up promptly until 1 day later.

Cytoskeletal molecules such as actin and microtubule play essential roles in T cell activation. Disruption of these molecules will impair T cell signaling, probably by inhibiting membrane molecule aggregation and rearrangement (22). Cytochalasin D (CD), a drug that interferes with actin cytoskeleton function, impaired the ability of 1E5 T cells to exhibit a polarized shape, an effect similar to that of POH (Fig. 1D). In contrast, when treated with colchicine, a drug that interferes with microtubule function, T cells still showed a polarized shape, although cell growth was inhibited at this concentration (Fig. 1E). These studies might imply that regulation of actin polymerization is involved in the disruption of 1E5 T cell polarity by POH.

Apoptosis of 1E5 and human T cells induced by POH. Since POH caused polarized-shape 1E5 T cells to round up and exhibit apoptosis-like morphology, we used flow cytometry to examine whether apoptosis occurred in a POH-treated cell population. Indeed, POH induced a dose-dependent apoptosis in 1E5 T cells. One-hour incubation of 1 mM POH induced apoptosis in ~10% of the cells incubated in the mammalian Ringer solution with glucose (Fig. 3). Following a 1-h incubation with 5 mM POH, almost all of the cells were stained with both annexin V and PI, a common characteristic of late apoptosis in cells. Adding farnesylpyrophosphate (FPP) or geranylgeranylpyrophosphate (GGPP) or both with POH did not prevent cell death. Removal of POH after 10 min incubation prevented further cell death (Fig. 3). Apoptosis was not detected within the first 6 h when the cells were treated with 1–5 mM POH in the complete culture medium. However, most of the cells were apoptotic 1 day later (data not shown), consistent with the results of cell morphology change.

POH also induced apoptosis in activated human T cells in a dose-dependent manner (Fig. 4). One-day incubation with 0.5 mM POH caused cell death (annexin V^+/PI^- and annexin V^+/PI^+) in 24% of activated human T cells in complete culture medium. POH also induced cell death in resting human T cells, although at much higher POH concentrations. About 26% of resting human T cells were stained with annexin V with 1-day incubation of 5 mM POH. This result makes POH more attractive, since an ideal immunosuppressive drug should affect activated T cells while sparing the resting ones.

$[Ca^{2+}]_i$ changes to POH treatment. Calcium plays important roles in T cell shape and motility (20). Sustained elevation of $[Ca^{2+}]_i$ is detrimental to cells and is often associated with cell death. Previously, we showed that 1E5 T cell shape and motility are extremely sensitive to changes in $[Ca^{2+}]_i$ (K_d = 200 nM) (20). At resting $[Ca^{2+}]_i$ (80 nM), most cells had a

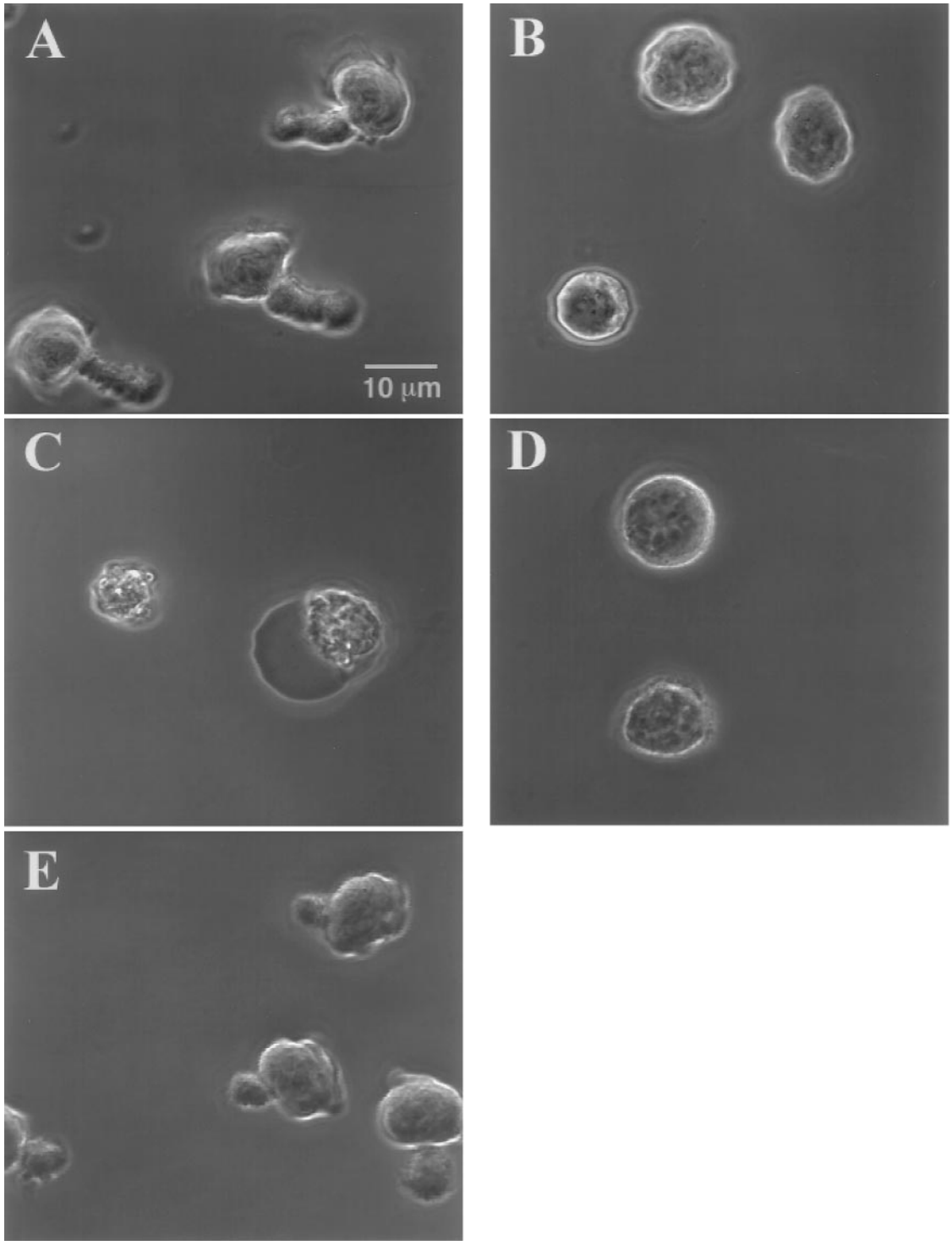

FIG. 1. Effects of POH, CD, and colchicine on cell shape and motility. (A) Before POH treatment, ~95% of 1E5 cells have a polarized shape, which is defined as a cell shape index >1.3. (B) POH treatment caused a decrease in the polarized-shape cell population. Nonpolarized cells with a shape index ~1.0–1.2 showed no motility. (C) 1E5 cells showed apoptosis-like morphology when incubated with 5 mM POH for 30 min. (D) CD effect (100 μM for 30 min) on 1E5 cell shape. (E) Colchicine effect (500 μM for 30 min) on 1E5 cell shape.

polarized shape with a shape index (the ratio of the long axis to the short) of ~1.3–2.0. When $[Ca^{2+}]_i$ was elevated, the cells rounded up with a shape index close to 1.0. The changes in cell shape index with $[Ca^{2+}]_i$ were reversible. Here, we recorded the shape index and $[Ca^{2+}]_i$ in single 1E5 T cells treated with

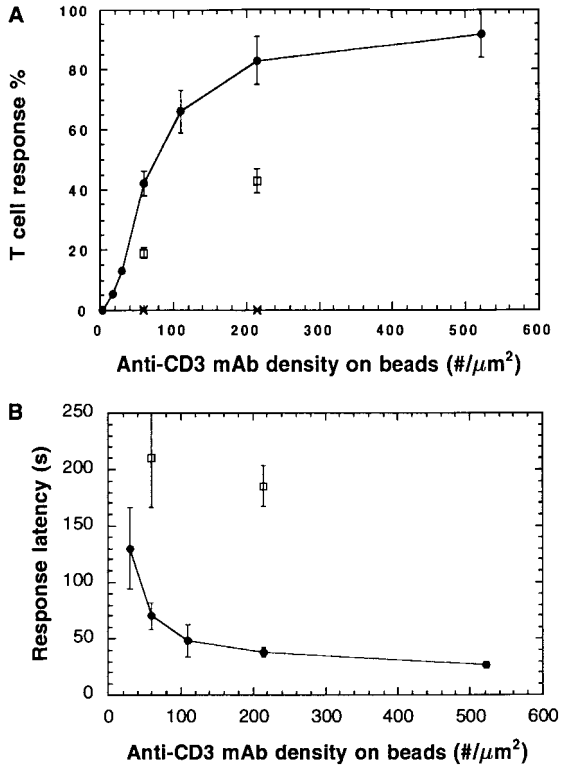

FIG. 2. Impairment of TCR-mediated $[Ca^{2+}]_i$ response by POH. (A) Calcium response percentage decreased by POH. 30 min incubation of 1 mM POH resulted in ~45% decrease in the polarized-shape population. Nonpolarized cells showed no calcium response to anti-CD3 mAb-coated bead stimulation at the leading edge (labeled ×). Within the polarized-shape population, the percentage of cells with calcium response to two different antibody–density bead stimulations (□) was consistently reduced by 50% compared with that of DMSO control (●). (B) Latency time increase of calcium response by POH treatment in 1E5 cells to anti-CD3 mAb-coated bead stimulation. POH incubation resulted in a decrease of the polarized-shape population. Within the polarized-shape population with POH treatment, the latencies of calcium response (□) have consistent 3-min increases, compared with those of DMSO control (●). Standard error bars shown in the figure are based on at least two independent experiments (n = 60 cells/point).

POH (Fig. 5). Interestingly, POH induced an initial $[Ca^{2+}]_i$ spike within seconds and cells rounded up. Within 2–5 min, $[Ca^{2+}]_i$ declined almost to the baseline level and the polarized shape of 1E5 cells recovered. After 10–15 min, $[Ca^{2+}]_i$ rose again and remained elevated. Shortly thereafter, cell plasma membrane blebbing occurred and accompanied the sustained $[Ca^{2+}]_i$ event (Fig. 5). These surface blebs were highly dynamic, giving the appearance of membrane boiling, which was characteristic of apoptosis, as reported previously (23, 24). Adding FPP or GGPP or both with POH had no effect on this scenario. The polarized shape of 1E5 cells did not recover once they were round, even when POH was removed after 10 min incubation (data not shown).

DISCUSSION

POH is a nontoxic, naturally occurring monoterpene. Previously, we showed that POH, a known protein isoprenylation inhibitor and anticancer agent, effectively inhibits human T cell proliferation and prevents acute and chronic rejection in a rat cardiac transplant model. In this report, we demonstrate that POH, at concentrations shown to have *in vitro* anticancer activity (3, 5), disrupts the polarized shape and motility of murine 1E5 T cells. POH also significantly impairs the cellular calcium response to anti-CD3 mAb stimulation. We further show that POH induces apoptosis in human T lymphocytes as well as in 1E5 T cells. Activated human T cells were as least 10-fold more sensitive to POH-induced cell death than resting T cells. A rise in $[Ca^{2+}]_i$ is associated with POH-induced shape change and apoptosis of 1E5 T cells. We propose that POH may act as an antirejection agent by disrupting T cell motility and TCR-mediated $[Ca^{2+}]_i$ signaling and by inducing apoptosis in activated T cells.

Our data provide the first evidence that POH induces apoptosis preferentially in activated human T cells, as well as in a murine 1E5 T cell line. POH has been shown to inhibit the isoprenylation of small 21- to 26-kDa proteins, including Ras and Ras-related proteins, in human-derived lymphoid and other cell lines, leading to the inhibition of cellular proliferation (3). This inhibition, once thought to be secondary to the inhibition of isoprenylation of the Ras superfamily of GTPases, may be caused by decreased levels of total Ras and Ras-related GTPases, as shown by Hohl *et al.* and Schulz *et al.* (4, 12). We have shown that POH has little toxicity on resting human T cells, whereas PHA-activated human T cells exposed to POH readily undergo apoptosis (Fig. 4). Gómez *et al.* studied the role of Ras in T cell proliferation and apoptosis and suggested that the cell proliferation is the consequence of a minimal number of molecular pathways involved in T cell activation (25). Incomplete signals may result in apoptotic cell death, instead of cell proliferation and effector functions. Thus, the inhibition of Ras by POH in PHA-treated T cells might cause incomplete signaling and programmed cell death.

Our results show that POH affects T cell motility and cytoskeletal dynamics that are essential in T cell activation and migration. Furthermore, POH impairs one of the important TCR-mediated early signaling events, the $[Ca^{2+}]_i$ response in T cells. Recently, Wülfing *et al.* reported an active, cytoskeletal mechanism that appears to drive receptor accumulation at the T cell–APC interface (26). Valitutti *et al.* demonstrated that cytochalasin D and C2 *Clostridium botulinum* toxin drugs that disrupt the actin cytoskeleton, induced a rapid block of $[Ca^{2+}]_i$ signaling, coincident with a block of the cyclic changes in T

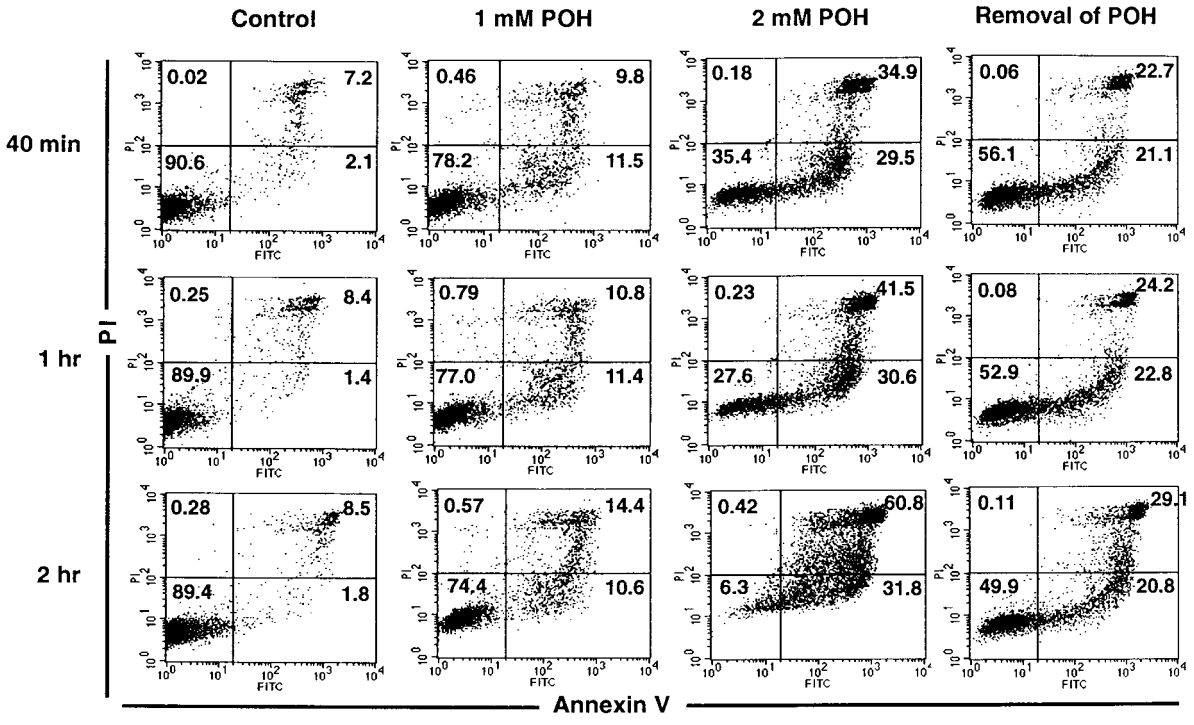

FIG. 3. POH-induced apoptosis in 1E5 T cells. After various times and concentrations of POH treatment, 1E5 cells were incubated with FITC-conjugated annexin V and propidium iodide and analyzed by FACScan. *X* axis, fluorescence level of FITC-conjugated annexin V; *Y* axis, fluorescence level of propidium iodide. Removal of 2 mM POH after 10 min incubation prevented further cell death.

cell shape after T cells made active interactions with specific antigen-presenting cells (22). The shape and motility are essential for T cells when one considers that lymphocytes adhere to cellular and extracellular matrices, squeeze through blood vessel fenestrations, and are usually activated in the packed cellular environment of lymph nodes (27). RhoA is a geranylgeranylated GTPase and a member of the small GTP-binding proteins of the Ras family. It regulates actin polymerization and thus cytoskeletal dynamics. POH has been shown to inhibit the geranylgeranylation of this GTPase (28). Our pharmacological data suggest that POH may affect the actin component of the cytoskeleton.

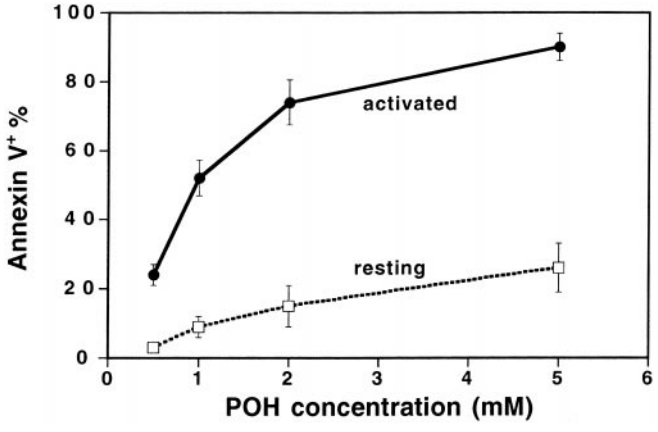

FIG. 4. Apoptosis induced by POH in human T cells measured by FACScan. Human peripheral blood T cells were activated with 5 μg/ml PHA for 3 days in complete culture medium, washed, and incubated with POH for 18 h before cell apoptosis analysis. POH also induced apoptosis in a smaller percentage of resting T cells. The baselines of cell death for the resting and activated human T cells incubated for 18 h without POH are 7 and 9%, respectively. Baseline-subtracted cell death percentages are shown. Standard errors are shown for FACScan runs of three independent experiments, ~10,000 cells/run.

An ideal antirejection agent should affect activated (alloresponsive) T cells while sparing the resting (nonreactive) ones. Our preclinical results showed that POH-treated animals maintained excellent graft function for greater than 75 days, even after cessation of treatment at day 30 (13). Treated animals exhibited normal activity and no signs of toxicity or infection. Furthermore, POH has beneficial anticancer and chemopreventive properties, while other immunosuppressants, such as cyclosporin A, may promote cancer (29). Recently, we and others have demonstrated that pravastatin, another isoprenylation inhibitor, was also able to inhibit T cell proliferation and decrease chronic rejection in cardiac and kidney transplant patients taking cyclosporin A (13, 30, 31). Our demonstration that POH induces apoptosis in activated T cells and disrupts T cell shape may explain its antirejection properties.

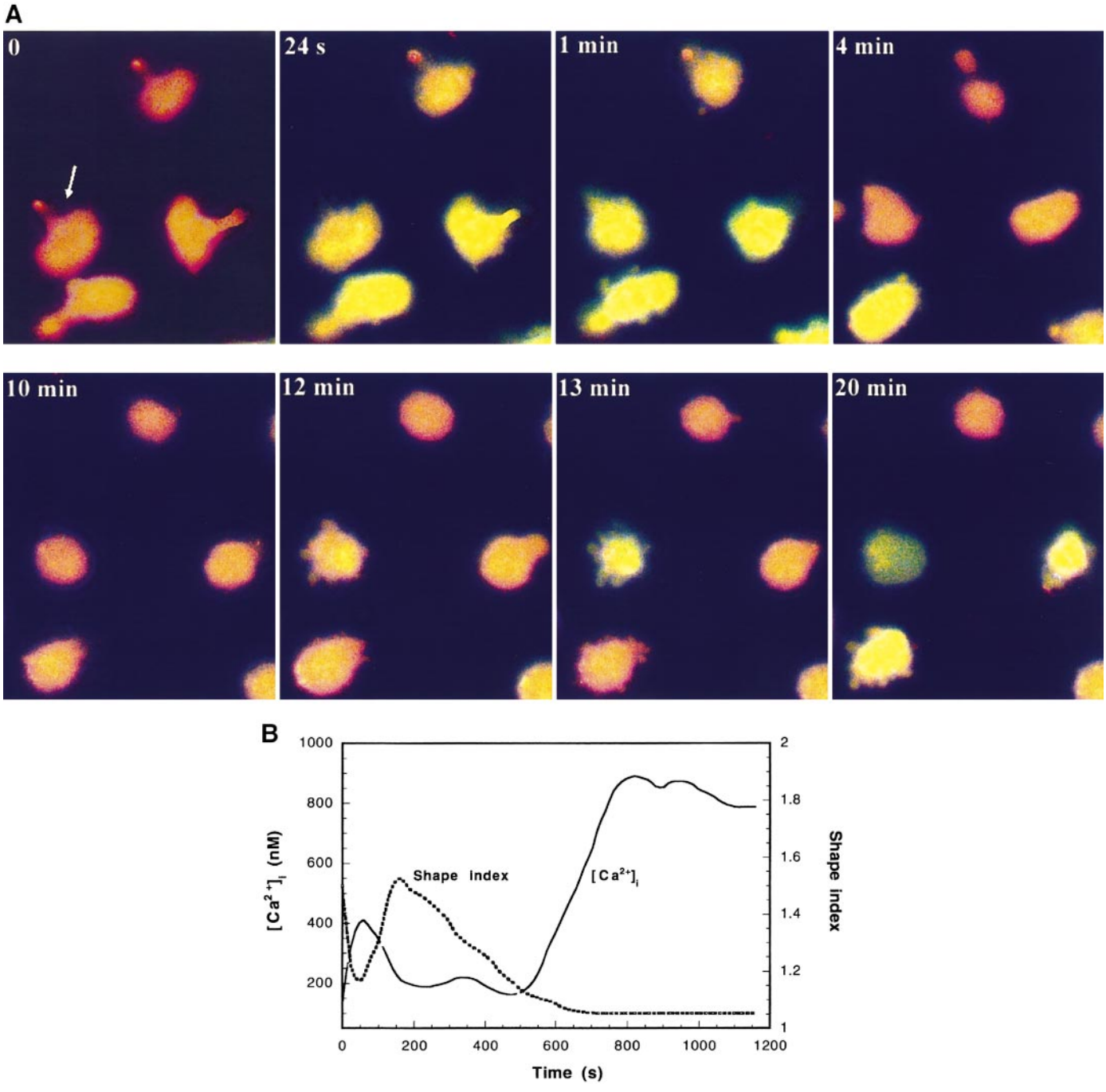

FIG. 5. POH-induced $[Ca^{2+}]_i$ rise (>80%, 45 of 52 cells from three independent experiments). (A) Bright field and fluorescence images are shown as an overlay. 1E5 T cells were preincubated with calcium indicators. Cells were settled on a heated stage (37°C) in Ringer solution/glucose and had a polarized shape before 2 mM POH was added to the cell solution at time 0. (B) Time course of $[Ca^{2+}]_i$ and the shape index for a typical cell, shown with an arrow in (A). $[Ca^{2+}]_i$ was estimated every 4 s.

ACKNOWLEDGMENTS

This work was supported by NIH Grants RR01192, LAMMP Biotechnology Resource Center (B.J.T.), and GM41514 (M.D.C.), the AOA Honor Medical Society, the Office of Naval Research (N00014-91-C-0134), and also in part by an unrestricted grant from Bristol Myers Squibb, Inc. We thank T. Krasieva and L. Forrest for excellent technical assistance.

REFERENCES

1. Schreiber, S. L., and Crabtree, G. R., The mechanism of action of cyclosporin A and FK506. *Immunol. Today* **13,** 136–142, 1992.
2. Min, D. I., and Monaco, A. P., Complications associated with immunosuppressive therapy and their management. *Pharmacotherapy* **11,** 119S–125S, 1991.

3. Crowell, P. L., Chang, R. R., Ren, Z., Elson, C. E., and Gould, M. N., Selective inhibition of isoprenylation of 21–26-kDa proteins by the anticarcinogen *d*-limonene and its metabolites. *J. Biol. Chem.* **266,** 17679–17685, 1991.
4. Hohl, R. J., and Lewis K., Differential effects of monoterpenes and lovastatin on RAS processing. *J. Biol. Chem.* **270,** 17508–17512, 1995.
5. NCI, DCPC chemoprevention branch and agent development committee, clinical development plan: *l*-Perillyl alcohol. *J. Cell. Biochem.* **26S,** 137–148, 1996.
6. Mills, J. J., Chari, R. S., Boyer, I. J., Gould, M. N., and Jirtle, R. L., Induction of apoptosis in liver tumors by the monoterpene perillyl alcohol. *Cancer Res.* **55,** 979–983, 1995.
7. Reddy, B. S., Wang, C. X., Samaha, H., Lubet, R., Steele, V. E., Kelloff, G. J., and Rao, C. V., Chemoprevention of colon carcinogenesis by dietary perillyl alcohol. *Cancer Res.* **57,** 420–425, 1997.
8. Lebowitz, P. F., and Prendergast, G. C., Non-Ras targets of farnesyltransferase inhibitors: Focus on Rho. *Oncogene* **17,** 1439–1445, 1998.
9. Downward, J., Graves, J. D., Warne, P. H., Rayter, S., and Cantrell, D. A., Stimulation of p21ras upon T-cell activation. *Nature* **346,** 719–723, 1990.
10. Izquierdo Pastor, M., Reif, K., and Cantrell, D., The regulation and function of p21ras during T-cell activation and growth. *Immunol. Today* **16,** 159–164, 1995.
11. Rayter, S., Woodrow, M., Lucas, S., Cantrell, D., and Downward, J., p21ras mediates control of IL-2 gene promoter function in T cell activation. *EMBO J.* **11,** 4549–4556, 1992.
12. Schulz, S., Reinhold, D., Schmidt, H., Ansorge, S., and Höllt, V., Perillic acid inhibits Ras/MAP kinase-driven IL-2 production in human T lymphocytes. *Biochem. Biophys. Res. Commun.* **241,** 720–725, 1997.
13. Si, M., Wei, X., Imagawa, D. K., Maggard, M., Ke, B., Wang, T., Meng, L., Kato, H., Spear, G., Coito, A., Kupiec-Wegilinski, J., Tromberg, B. J., and Busuttil, R. W., Isoprenylation inhibitors pravastatin and perillyl alcohol as immunosuppressive agent. *Transplantation,* in press, 2000.
14. Adorini, L., Sette, A., Buus, S., Grey, H. M., Darsley, M., Lehman, P. V., Doria, G., Nagy, Z. A., and Appella, E., Interaction of an immunodominant epitope with Ia molecules in T-cell activation. *Proc. Natl. Acad. Sci. USA* **85,** 5181–5185, 1988.
15. Hess, S. D., Oortgiesen, M., and Cahalan, M. D., Calcium oscillations in human T and natural killer cells depend upon membrane potential and calcium influx. *J. Immunol.* **150,** 2620–2633, 1993.
16. Berns, M. W., Aist, J. R., Wright, W. H., and Liang, H., Optical trapping in animal and fungal cells using a tunable, near-infrared titanium–sapphire laser. *Exp. Cell Res.* **198,** 375–378, 1992.
17. Liang, H., Vu, K. T., Krishnan, P., Trang, T., Shin, D., Kimel, S., and Berns, M. W., Wavelength dependence of cell cloning efficiency after optical trapping. *Biophys. J.* **70,** 1529–1533, 1996.
18. Grynkiewicz, G., Poenie, M., and Tsien, R. Y., A new generation of Ca^{2+} indicators with greatly improved fluorescence properties. *J. Biol. Chem.* **260,** 3440–3450, 1985.
19. Donnadieu, E., Cefai, D., Tan, Y. P., Paresys, G., Bismuth, G., and Trautmann, A., Imaging early steps of human T cell activation by antigen-presenting cells. *J. Immunol.* **148,** 2643–2653, 1992.
20. Negulescu, P. A., Krasieva, T. B., Khan, A., Kerschbaum, H. H., and Cahalan, M. D., Polarity of T cell shape, motility, and sensitivity to antigen. *Immunity* **4,** 421–430, 1996.
21. Wei, X., Tromberg, B. J., and Cahalan, M. D., Mapping the sensitivity of T cells with an optical trap: Polarity and minimal number of receptors for Ca^{2+} signaling. *Proc. Natl. Acad. Sci. USA* **96,** 8471–8476, 1999.
22. Valitutti, S., Dessing, M., Aktories, K., Gallati, H., and Lanzavecchia, A., Sustained signaling leading to T cell activation results from prolonged T cell receptor occupancy: Role of T cell actin cytoskeleton. *J. Exp. Med.* **181,** 577–584, 1995.
23. Martikainen, P., Kyprianou, N., Tucker, R. W., and Isaacs, J. T., Programmed death of nonproliferating androgen-independent prostatic cancer cells. *Cancer Res.* **51,** 4693–4700, 1991.
24. Furuya, Y., Lundmo, P., Short, A. D., Gill, D. L., and Isaacs, J. T., The role of calcium, pH, and cell proliferation in the programmed (apoptotic) death of androgen-independent prostatic cancer cells induced by thapsigargin. *Cancer Res.* **54,** 6167–6175, 1994.
25. Gómez, J., Martínez, C., Fernández, B., García, A., and Rebollo, A., Ras activation leads to cell proliferation or apoptotic cell death upon interleukin-2 stimulation or lymphokine deprivation, respectively. *Eur. J. Immunol.* **27,** 1610–1618, 1997.
26. Wülfing, C., and Davis, M. M., A receptor/cytoskeletal movement triggered by costimulation during T cell activation. *Science* **282,** 2266–2269, 1998.
27. Springer, T. A., Traffic signals for lymphocyte recirculation and leukocyte emigration: The multistep paradigm. *Cell* **76,** 301–314, 1994.
28. Ren, Z., Elson, C. E., and Gould, M. N., Inhibition of type I and type II geranylgeranyl-protein transferases by the monoterpene perillyl alcohol in NIH3T3 cells. *Biochem. Pharm.* **54,** 113–120, 1997.
29. Hojo, M., Morimoto, T., Maluccio, M., Asano, T., Morimoto, K., Lagman, M., Shimbo, T., and Suthanthiran, M., Cyclosporine induces cancer progression by a cell-autonomous mechanism. *Nature* **397,** 530–534, 1999.
30. Kobashigawa, J. A, Katznelson, S., Laks, H., Johnson, J. A., Yeatman, L., Wang, X. M., Chia, D., Terasaki, P. I., Sabad, A., Cogert, G. A., *et al.,* Effect of pravastatin on outcomes after cardiac transplantation. *New Engl. J. Med.* **333,** 621–627, 1995.
31. Katznelson, S., Wilkinson, A. H., Kobashigawa, J. A., Wang, X. M., Chia, D., Ozawa, M., Zhong, H. P., Hirata, M., Cohen, A. H., Teraski, P. I., *et al., Transplantation* **61,** 1469–1474, 1996.